



**High performance of symmetric micro supercapacitors  
based on silicon nanowires using  
N-methyl-N-propylpyrrolidinium  
bis(trifluoromethylsulfonyl)imide as electrolyte**

David Aradilla, P. Gentile, Gérard Bidan, Vanesa Ruiz, Pedro Gómez-Romero,  
Thomas J.S. Schubert, Hülya Sahin, Elzbieta Frackowiak, Saïd Sadki

► **To cite this version:**

David Aradilla, P. Gentile, Gérard Bidan, Vanesa Ruiz, Pedro Gómez-Romero, et al.. High performance of symmetric micro supercapacitors based on silicon nanowires using N-methyl-N-propylpyrrolidinium bis(trifluoromethylsulfonyl)imide as electrolyte. 2014. <cea-01053082>

**HAL Id: cea-01053082**

**<https://hal-cea.archives-ouvertes.fr/cea-01053082>**

Submitted on 29 Jul 2014

**HAL** is a multi-disciplinary open access archive for the deposit and dissemination of scientific research documents, whether they are published or not. The documents may come from teaching and research institutions in France or abroad, or from public or private research centers.

L'archive ouverte pluridisciplinaire **HAL**, est destinée au dépôt et à la diffusion de documents scientifiques de niveau recherche, publiés ou non, émanant des établissements d'enseignement et de recherche français ou étrangers, des laboratoires publics ou privés.



Available online at [www.sciencedirect.com](http://www.sciencedirect.com)

ScienceDirect

journal homepage: [www.elsevier.com/locate/nanoenergy](http://www.elsevier.com/locate/nanoenergy)

RAPID COMMUNICATION

# High performance of symmetric micro-supercapacitors based on silicon nanowires using N-methyl-N-propylpyrrolidinium bis(trifluoromethylsulfonyl)imide as electrolyte

David Aradilla<sup>a,b</sup>, Pascal Gentile<sup>b,\*</sup>, Gérard Bidan<sup>c</sup>, Vanesa Ruiz<sup>d</sup>, Pedro Gómez-Romero<sup>d</sup>, Thomas J.S. Schubert<sup>e</sup>, Hülya Sahin<sup>e</sup>, Elzbieta Frackowiak<sup>f</sup>, Saïd Sadki<sup>a,\*</sup>

<sup>a</sup>LEMOH/SPRAM/UMR 5819 (CEA,CNRS, UJF), CEA/INAC Grenoble, France

<sup>b</sup>SiNaPS Lab.-SP2M, UMR-E CEA/UJF, CEA/INAC Grenoble, France

<sup>c</sup>INAC/Dir, CEA/INAC Grenoble, 17 rue des Martyrs, 38054 Grenoble, France

<sup>d</sup>ICN2 (CSIC-ICN), Campus UAB, 08193 Bellaterra, Barcelona, Spain

<sup>e</sup>IOLITEC Ionic Liquids Technologies GmbH, Salzstrasse 184, 74076 Heilbronn, Germany

<sup>f</sup>Poznan University of Technology, Institute of Chemistry and Technical Electrochemistry, Piotrowo 3, 60965 Poznan, Poland

Received 8 April 2014; received in revised form 12 June 2014; accepted 1 July 2014

## KEYWORDS

Silicon nanowires;  
Micro-supercapacitors;  
Ionic liquids;  
Electrochemical energy storage;  
Chemical vapor deposition

## Abstract

**Q3 Q2** This work describes the development and performance of a symmetric micro-supercapacitor made of nanostructured electrodes based on silicon nanowires (SiNWs) deposited using chemical vapor deposition (CVD) on silicon substrates. The performance of the SiNWs micro-supercapacitor employing an aprotic ionic liquid (N-methyl-N-propylpyrrolidinium bis(trifluoromethylsulfonyl)imide) (PYR<sub>13</sub>TFSI) as an electrolyte was able to deliver a maximal power density of 182 mW cm<sup>-2</sup> and a specific energy of 190 μJ cm<sup>-2</sup> operating at a wide cell voltage of 4 V with a quasi-ideal capacitive behavior. The lifetime of the device exhibited a remarkable electrochemical stability retaining 75% of the initial capacitance after several million galvanostatic charge-discharge cycles at a high current density of 1 mA cm<sup>-2</sup>. Furthermore,

\*Corresponding authors.

E-mail addresses: [pascal.gentile@cea.fr](mailto:pascal.gentile@cea.fr) (P. Gentile), [said.sadki@cea.fr](mailto:said.sadki@cea.fr) (S. Sadki).

<http://dx.doi.org/10.1016/j.nanoen.2014.07.001>

2211-2855/© 2014 Published by Elsevier Ltd.

a coulombic efficiency of approximately 99% was obtained after galvanostatic cycling test without structural degradation on the morphology of SiNWs.

© 2014 Published by Elsevier Ltd.

## Introduction

Over the past years new nanostructured materials, as for example nanowires, have emerged as promising materials in different technological applications such as photovoltaic cells or energy storage devices [1]. Within this context, SiNWs have attracted a great attention in the field of batteries [2] and supercapacitors [3]. Specifically, micro-supercapacitor electrodes made of SiNWs [3-7] and silicon carbide nanowires (SiCNWs) [8-10] can be considered as one of the next generation energy storage devices according to their interesting properties in terms of stable cycling life, fast charging-discharging rate and high power density. Additionally, SiNWs can be integrated in the Si-based microelectronics industry for the building and miniaturization of micro-electronic devices (e.g. diodes or transistors), [11] which represents an important advantage compared with micro-supercapacitor electrodes based on nanostructured carbon. Recently, SiNWs grown by using CVD on silicon substrates were proved as excellent micro-supercapacitors in propylene carbonate (PC) based electrolyte [3-5]. In order to improve the performance of SiNWs as micro-supercapacitor electrodes, different strategies have already been reported by using metallic oxides (NiO) [12,13] or cermets (SiC) [14] in the presence of aqueous electrolytes (KOH or KCl respectively). However, one of the most important drawbacks of aqueous electrolytes and organic solvents (e.g. PC or acetonitrile) concerns their narrow voltage cell ( $V$ ) (e.g.  $\sim 1.3$  V for aqueous electrolyte and  $\sim 2.7$  V for organic solvents), which limits the specific energy ( $E=1/2CV^2$ ) where  $C$  is the capacitance and  $V$  is the cell potential and the maximal power density ( $P=V^2/4ESR$ ) where  $ESR$  is the equivalent series resistance. Both properties power and energy density play an important role in the success of new electrochemical capacitors. Currently, ionic liquids (ILs) have provided wide electrochemical windows ( $>4$  V) and high thermal stability ( $>300$  °C), [15] as a consequence they have been used as alternative electrolytes in supercapacitors based on carbon electrodes [16-20]. Nowadays, the performance of SiNWs as micro-supercapacitors in a device configuration has been carried out mainly in a PC solution containing 1 M tetraethylammonium tetrafluoroborate [3-5] ( $\text{NEt}_4\text{BF}_4$ ) as an electrolyte operating at a working voltage of 1.0 and 1.2 V. These devices exhibit energy [3] and maximal power density [4,5] values ranging from 0.8 to 10.3 nWh  $\text{cm}^{-2}$  and from 1.4 to 1.6 mW  $\text{cm}^{-2}$  using SiNWs with different lengths and diameters on silicon substrates. In this way, to the best of our knowledge scarce works have been reported according to the performance of SiNWs as micro-supercapacitors (e.g. 2-electrode configuration) in the presence of ILs (1-ethyl-3-methylimidazolium bis(trifluoromethylsulfonyl)imide, EMIM TFSI) [7,21]. Thus, both studies were reported using a

narrow cell voltage of  $\sim 1.5$  V. In this study, we present a complete and detailed characterization of symmetric SiNWs micro-supercapacitors operating at a wide cell voltage of 4 V using N-methyl-N-propylpyrrolidinium bis(trifluoromethylsulfonyl)imide (Scheme 1) as an electrolyte owing to its moderate viscosity and wide voltage stability window [22,23]. Besides high values in terms of energy (190  $\mu\text{J cm}^{-2}$ ) and maximal power density (182 mW  $\text{cm}^{-2}$ ) found in this IL compared with PC [3-5] and EMIM TFSI [21] the results prove that supercapacitor electrodes based on SiNWs in a device configuration present an excellent stability after millions of galvanostatic charge-discharge cycles. Therefore, SiNWs can be found as promising and alternative materials to commercial supercapacitors based on carbon electrodes.

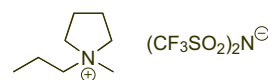
## Materials and methods

### Materials and reagents

Highly n-doped Si (111) substrates (doping level:  $5 \times 10^{18}$  doping atoms  $\text{cm}^{-3}$ ) and resistivity less than 0.005  $\Omega \text{cm}$  were used as the substrate for SiNW growth. Gold colloid solution (50 nm) was purchased from British BioCell. N-methyl-N-propylpyrrolidinium bis(trifluoromethylsulfonyl)imide was purchased from IOLITEC (Ionic Liquids Technologies GmbH, Germany) and used without further purification.

### Growth of SiNWs

SiNWs electrodes with a length of approximately 50  $\mu\text{m}$  and a diameter of 50 nm were grown in a CVD reactor (Easy-Tube3000 First Nano, a Division of CVD Equipment Corporation) by using the vapor-liquid-solid (VLS) method via gold catalysis on highly doped n-Si (111) substrate. Gold colloids with size of 50 nm were used as catalysts,  $\text{H}_2$  as carrier gas, silane ( $\text{SiH}_4$ ) as silicon precursor, phosphine ( $\text{PH}_3$ ) as n-doping gas and HCl as additive gas. The use of HCl has been proved to reduce the gold surface migration and improve the morphology of SiNWs [24,25]. Prior to the growth, wafer surface was cleaned by successive dipping in acetone, isopropanol and Caro ( $\text{H}_2\text{SO}_4:\text{H}_2\text{O}_2$ , 3:1 v/v) solutions in order to remove organic impurities, after that, the substrates were dipped in HF 10% and  $\text{NH}_4\text{F}$  solution to remove the native oxide layer. Finally, the gold catalyst was deposited on the surface. The deposition was carried out using HF 10% from an aqueous gold colloid solution.



**Scheme 1** Chemical structure of N-methyl-N-propylpyrrolidinium bis(trifluoromethylsulfonyl)imide (PYR<sub>13</sub>TFSI).

The growth was performed at 600 °C, under 6 Torr total pressure, with 40 sccm (standard cubic centimeters) of SiH<sub>4</sub>, 100 sccm of PH<sub>3</sub> gas (0.2% PH<sub>3</sub> in H<sub>2</sub>), 100 sccm of HCl gas and 700 sccm of H<sub>2</sub> as supporting gas for 32 min. The doping level (dl) of the SiNWs was managed by the pressure ratio: dopant gas/SiH<sub>4</sub>, which was evaluated in previous works (dl:  $4 \times 10^{19} \text{ cm}^{-3}$ ) [24].

## Design of the micro-supercapacitor

Symmetric micro-supercapacitors were designed from nanostructured electrodes made of SiNWs ( $L=50 \mu\text{m}$ ,  $\varnothing=50 \text{ nm}$ ) with a surface of  $1 \text{ cm}^2$ . A homemade two-electrode supercapacitor cell was built by assembling two nanostructured electrodes separated by a Whatman glass fiber paper separator soaked with the electrolyte (PYR<sub>13</sub> TFSI).

## Electrochemical characterization of micro-supercapacitors

Cyclic voltammetry (CV) curves and galvanostatic charge-discharge cycles were performed between 0 and 4 V using different scan rates ( $0.2\text{--}5 \text{ V s}^{-1}$ ) and current densities ( $0.1\text{--}1 \text{ mA cm}^{-2}$ ) respectively. Electrochemical impedance spectroscopy (EIS) measurements were performed using a sinusoidal signal of  $\pm 10 \text{ mV}$  amplitude and a frequency range from 100 kHz to 100 mHz. The electrochemical stability of the device was obtained by performing galvanostatic charge-discharge cycles over  $8 \times 10^6$  cycles at a current density of  $1 \text{ mA cm}^{-2}$  in the potential range from 0 to 4 V. The voltage hold test was carried out using a similar procedure previously reported [26,27]. The full cell was charged up to a voltage of 4 V and kept there for 5 h before five galvanostatic charge-discharge cycles at a current density of  $1 \text{ mA cm}^{-2}$  between 0 and 4 V, which allowed to determine the capacitance during the test. This procedure was repeated 60 times, resulting in a holding time of 300 h. All measurements were carried out using PYR<sub>13</sub> TFSI as an electrolyte in an argon-filled glove box with oxygen and water levels less than 1 ppm at room temperature.

## Morphological characterization

The morphology of the resulting SiNWs before and after electrochemical testing was examined by using a ZEISS Ultra 55 scanning electron microscope operating at an accelerating voltage of 10 kV. SiNWs were rinsed with acetone and isopropanol to ensure removal of excess electrolyte after electrochemical testing.

## Results and discussion

Figure 1a and b displays general and magnified SEM images about the growth of SiNWs onto silicon substrates by using the VLS method. It can be noted that a high density of SiNWs appears by using this method reflecting an average nanowire density of  $2.51 \times 10^8 \pm 9.25 \times 10^7 \text{ nanowires cm}^{-2}$ . The SiNWs density was estimated by counting the number of gold colloids per  $\text{cm}^2$  on several SEM images. Gold colloids

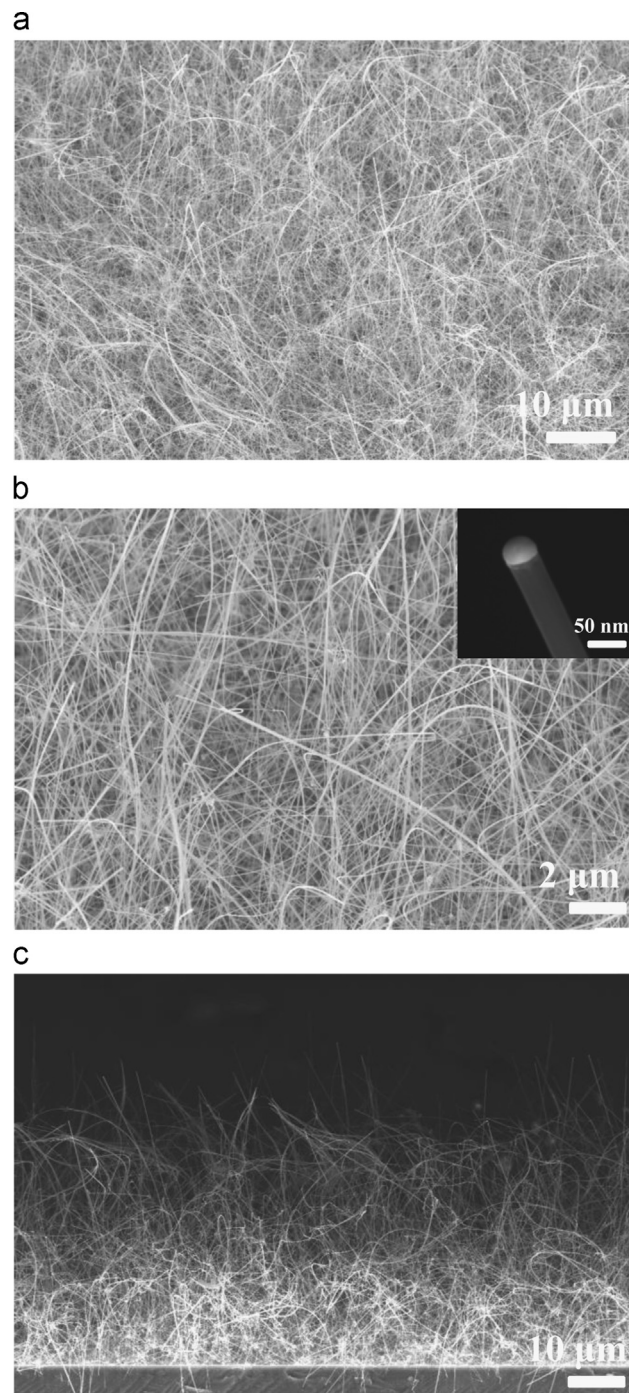


**Figure 1** (a) and (b) Low and high magnification SEM images of the morphology of SiNWs with gold colloids recorded at 45° tilted angle. Inset shows the gold tip at the top of SiNWs. (c) Cross sectional view of SiNWs. Scale bar: 10  $\mu\text{m}$ .

were kept on the top of SiNWs as depicted in Figure 1b (inset) because no influence on the electrochemical behavior was reported in previous studies [5]. The overall length of the SiNWs was found to be  $50 \mu\text{m} \pm 83 \text{ nm}$  according to the cross-section view depicted in Figure 1c. The diameter of SiNWs was estimated to be 50 nm as illustrated in Figure 1b (inset).



The electrochemical properties of the micro-supercapacitor device were evaluated by CV, galvanostatic charge-discharge curves and EIS techniques. Figure 2a shows the CV curves at different scan rates from  $0.2 \text{ V s}^{-1}$  to  $5 \text{ V s}^{-1}$  within a large electrochemical window of 4 V. The shape of the voltammetric curves is rectangular presenting a quasi-ideal capacitive behavior even at very high scan rates. According to this feature, voltammetric capacitive

currents are directly proportional to the scan rate of CV (Figure 2b) which demonstrates a negligible ohmic drop in the electrolyte bulk and no redox peaks between the electrodes and the electrolyte were detected. Thus, these results indicate excellent capacitive behavior of the SiNWs in a 2-electrode device configuration. Galvanostatic charge-discharge curves at different current densities were recorded in Figure 2c, the curves show a nearly symmetrical

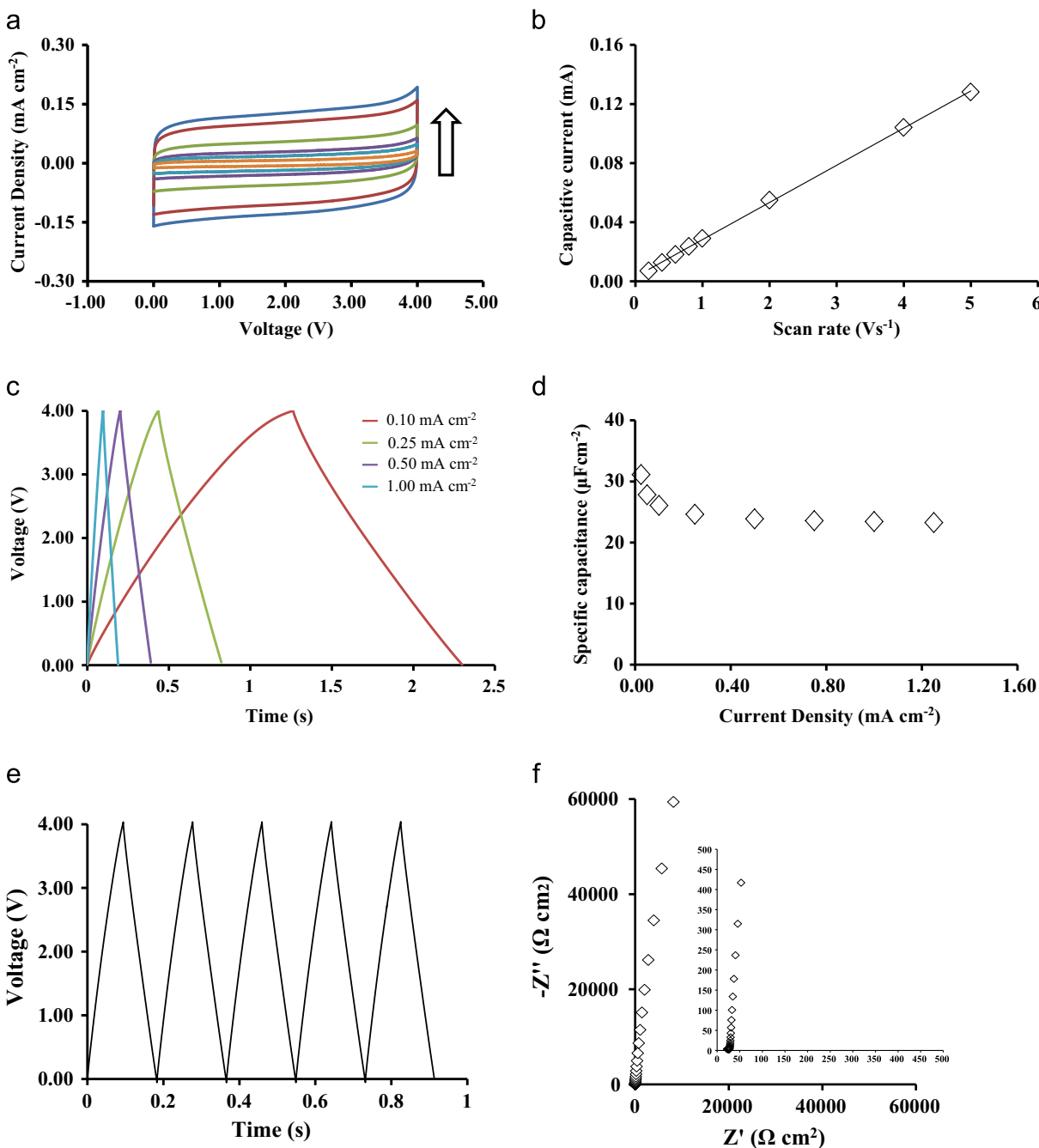


**Figure 2** Characterization of SiNWs micro-supercapacitors. (a) Cyclic voltammograms at different scan rates (0.2, 0.6, 1.0, 2.0, 4.0 and  $5.0 \text{ V s}^{-1}$  respectively). Arrow indicates the increase of scan rate. (b) Evolution of the capacitive current versus scan rate. (c) Charge-discharge cycles using different current densities ( $0.05\text{-}1 \text{ mA cm}^{-2}$ ). (d) Capacitance as a function of current densities. (e) The first five galvanostatic charge-discharge cycles at a current density of  $1 \text{ mA cm}^{-2}$  between 0 and 4 V. (f) Nyquist plot measured at 0 V after the conditions described in (e). The impedances were measured using a frequency range from 100 kHz to 100 mHz. Inset shows magnified high frequency region.

shape with linear slopes reflecting a pure capacitive behavior originating from the effective ion adsorption at the electrolyte-electrode interface. Galvanostatic charge-discharge measurements were used to calculate the specific capacitance of the device according to this equation:

$$SC = \frac{I \Delta t}{\Delta V A} \quad (1)$$

where  $SC$  ( $\mu\text{F cm}^{-2}$ ) is the specific capacitance of the micro-supercapacitor,  $I$  ( $\mu\text{A}$ ) corresponds to the discharge current,  $\Delta V$  (V) is the potential change within the discharge time  $\Delta t$  (s), and  $A$  ( $\text{cm}^2$ ) refers to the area of the electrodes ( $1 \text{ cm}^2$ ). As it can be seen in Figure 2d capacitance values decrease when the current density increases reaching a plateau at current densities higher than  $0.4 \text{ mA cm}^{-2}$ . According to Eq. (1) a value of  $\sim 23 \mu\text{F cm}^{-2}$  was achieved in the plateau region which leads to a density energy value of  $\sim 190 \mu\text{J cm}^{-2}$  ( $0.053 \mu\text{Wh cm}^{-2}$ ). Thus, capacitance and energy values of  $23.42 \mu\text{F cm}^{-2}$  and  $187.36 \mu\text{J cm}^{-2}$  were obtained from the curves recorded in Figure 2e at a current density of  $1 \text{ mA cm}^{-2}$ . Energy densities calculated in this work were found higher than previous results based on similar conditions of the SiNWs growth (e.g.  $L=50 \text{ nm}$ ;  $\varnothing=20\text{-}200 \text{ nm}$ ) [3] performed in a PC solution containing  $1 \text{ M NET}_4\text{BF}_4$  as electrolyte ( $E=37 \mu\text{J cm}^{-2}/0.010 \mu\text{Wh cm}^{-2}$ ) operating at a cell voltage of  $1.2 \text{ V}$ . Therefore, an enhancement of 80% in terms of energy density was found using  $\text{PYR}_{13}\text{TFSI}$  as an electrolyte, which allowed an enlargement of the electrochemical window up to  $4 \text{ V}$ . Figure 2f presents the Nyquist plot of SiNWs supercapacitors where a straight line in the low frequency is shown. The vertical profile at low frequencies indicates pure capacitive behavior, which is associated with the diffusion of ions into the structure. In addition, symmetrical charge-discharge curves represented in Figure 2e reflect negligible IR drop suggesting a very low ESR, thus, EIS analysis obtained from Figure 2f (inset) allowed an estimation of  $22 \Omega \text{ cm}^2$  for ESR leading to a maximal power density ( $P^{\text{max}}$ ) of  $182 \text{ mW cm}^{-2}$  at a cell voltage of  $4 \text{ V}$  for the device. This result represents an outstanding improvement in the maximal power density as compared with previous studies of SiNWs of  $10 \mu\text{m}$  and  $20 \mu\text{m}$  in length (e.g.  $P^{\text{max}}$ :  $1.6$  and  $1.4 \text{ mW cm}^{-2}$  respectively) [4,5]. In this context, according to the literature other micro-supercapacitors based on carbon were performed on silicon substrates [28] showing a  $P^{\text{max}}$  value of  $34.4 \text{ mW cm}^{-2}$  with an ESR value of  $45.4 \Omega \text{ cm}^2$  or more recently, onion-like carbon (OLC) based micro-supercapacitors exhibited a  $P^{\text{max}}$  value of  $240 \text{ mW cm}^{-2}$  using an eutectic mixture of ionic liquids [18]. These values are similar or smaller than the experimental data obtained in this work. Our results demonstrate that SiNWs in the presence of ILs can be considered as an alternative material to carbon electrodes for portable electronic devices due to the improvement of the maximal power density.

The EIS technique is also a powerful tool in order to evaluate the capacitive behavior of micro-supercapacitor. Thus, the imaginary part of the complex capacitance versus frequency can be obtained according to the following equation [29]:

$$C''(\omega) = \frac{Z'(\omega)}{\omega |Z(\omega)|^2} \quad (2)$$

where  $C''(\omega)$  is the imaginary part of the capacitance,  $Z(\omega)$  is the impedance,  $Z'(\omega)$  is the real part of the impedance and  $\omega=2\pi f$  where  $f$  corresponds to the frequency. The  $C''(\omega)$  corresponds to an energy dissipation by an irreversible process that can lead to a hysteresis [29].

Figure 3 shows the evolution of  $C''$  versus frequency for the SiNWs micro-supercapacitor. Another important property on the performance of micro-supercapacitors is related with the relaxation time constant of the device ( $\tau_0$ ). This parameter is defined as the minimum time needed to discharge all the energy from the device with an efficiency of more than 50% [30]. From the plot displayed in Figure 3, the time constant was evaluated using the following relation ( $\tau_0=1/f_0$ ), which was calculated to be  $3.51 \text{ ms}$ . This value was found lower than other micro-supercapacitors reported in the literature based on carbon electrodes (e.g. values ranging from  $26$  to  $700 \text{ ms}$ ) [31]. Therefore, SiNWs electrodes in  $\text{PYR}_{13}\text{TFSI}$  as electrolyte possess a great potential for the instantaneous delivery of high power.

The Ragone plot in Figure 4 was used in order to determine the energy density ( $E$ ,  $\text{mJ cm}^{-2}$ ) and power density ( $P$ ,  $\text{mW cm}^{-2}$ ) of SiNWs micro-supercapacitors according to the following equations:

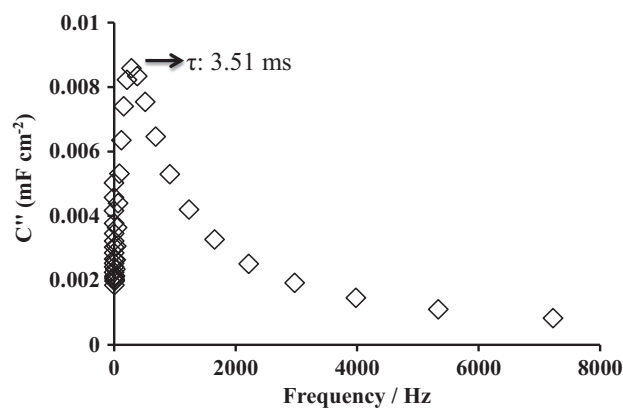


Figure 3 Evolution of the imaginary capacitance versus frequency for SiNWs micro-supercapacitor. The relaxation time constant ( $\tau_0$ ) of the device is indicated in the plot using an arrow.

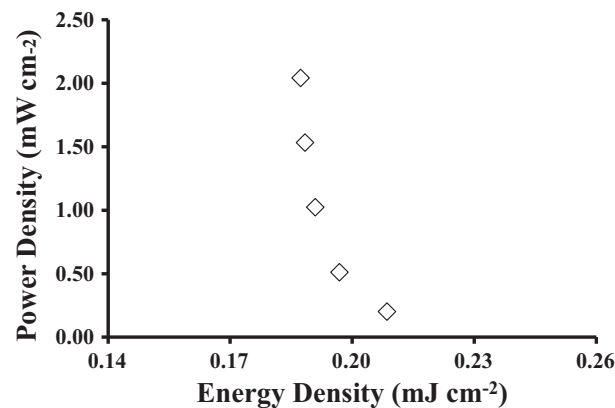
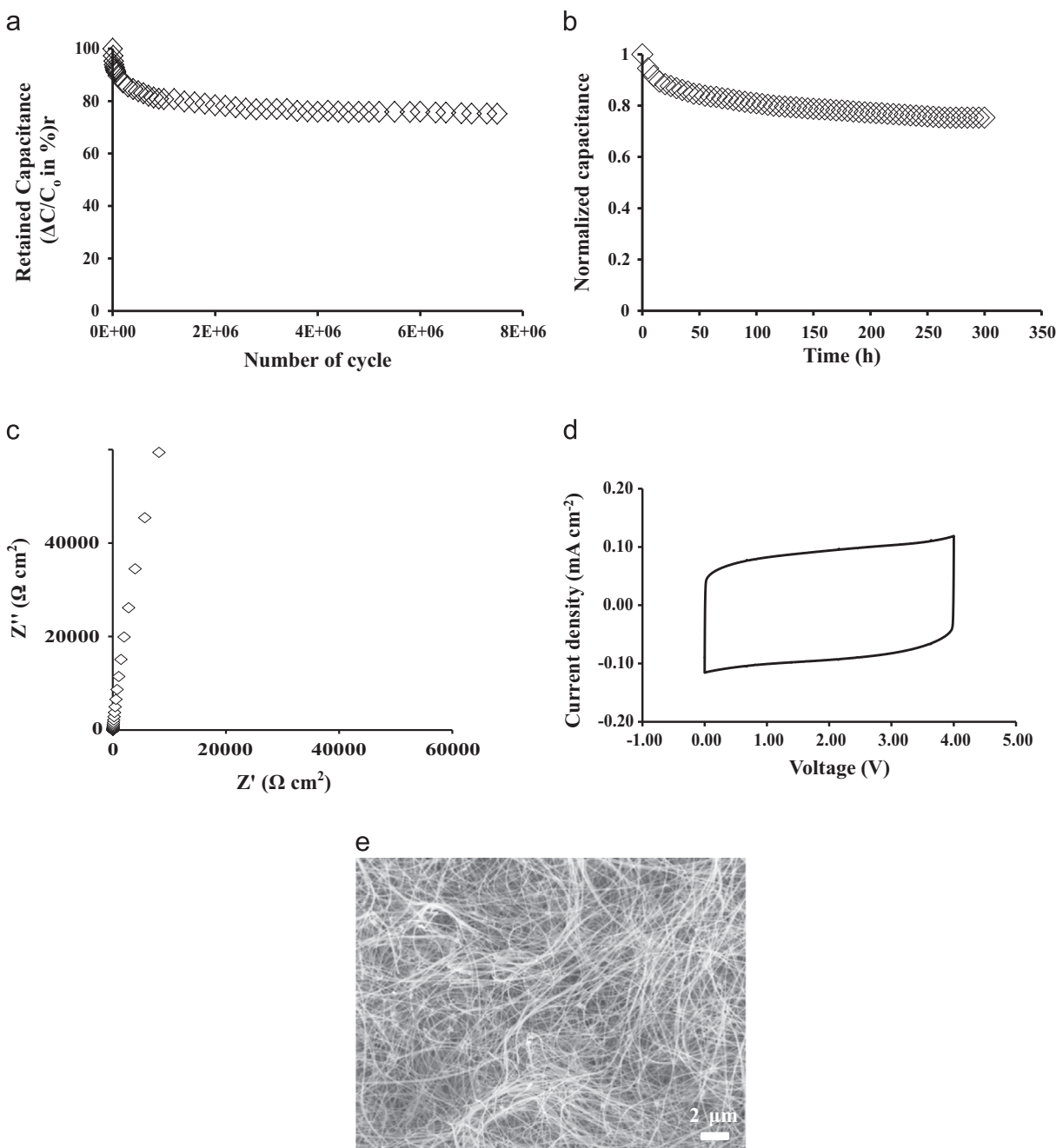


Figure 4 The Ragone plot per area for SiNWs micro-supercapacitors calculated by varying the discharging current density of  $0.1\text{-}1 \text{ mA cm}^{-2}$ .



**Figure 5** (a) Lifetime testing of the SiNWs micro-supercapacitors performed using  $8 \times 10^6$  complete charge discharge cycles at a current density of  $1 \text{ mA cm}^{-2}$  between 0 and 4 V. (b) Constant voltage hold test for a SiNWs micro-supercapacitor device using a cell voltage of 4 V. (c) Cyclic voltammogram after  $8 \times 10^6$  charge-discharge curves at a scan rate of  $5 \text{ V s}^{-1}$ . (d) Nyquist plots measured at 0 V after  $8 \times 10^6$  charge-discharge curves using a frequency range from 100 kHz to 100 mHz. (e) SEM micrographs of SiNWs after cycling under the conditions described in (a) at  $45^\circ$  tilted angle.

$$E = \frac{1}{2} SC \Delta V^2 \quad (3)$$

$$P = \frac{E}{\Delta t} \quad (4)$$

The Ragone plot increases rapidly with power density due to the fast voltage decay during discharge as shown in Figure 3. Power density values range from 1 to  $2 \text{ mW cm}^{-2}$

at current densities higher than  $0.5 \text{ mA cm}^{-2}$  and fast time constants of the device. These values obtained in the Ragone plot were compared with other supercapacitor systems. Within this context, supercapacitors based on fiber carbon [32,33] electrodes exhibited a power density value of  $0.56 \text{ mW cm}^{-2}$  and  $1 \text{ mW cm}^{-2}$ . Again, the results showed excellent performance of SiNWs compared with carbon electrodes as supercapacitors. In terms of energy



density, values of approximately  $0.19 \text{ mJ cm}^{-2}$  were calculated for the same range of current densities ( $0.5\text{--}1 \text{ mA cm}^{-2}$ ).

Electrochemical stability is an important key factor on the performance of supercapacitor devices. In this work, stability of the device was evaluated by repeating galvanostatic charge-discharge cycling between 0 and 4 V at a current density of  $1 \text{ mA cm}^{-2}$  for several million cycles. The percent of retained capacitance as a function of the cycle number is shown in Figure 5a. After  $8 \times 10^6$  charge-discharge cycles only  $\sim 25\%$  of the initial capacitance was found to be lost. More importantly, most of the degradation of the initial performance of the device occurs during the first 100,000 cycles according to the silicon oxidation, after which the system showed stabilization, reaching a plateau-like profile. This characteristic indicates that the micro-supercapacitor based on SiNWs demonstrates a remarkable stability and lifetime after millions of charge-discharge cycles in the presence of  $\text{PYR}_{13}\text{TFSI}$ . According to this data, the electrochemical stability of the device shows an excellent interaction between the electrodes (SiNWs) and the electrolyte ( $\text{PYR}_{13}\text{TFSI}$ ). Figure 5b shows the results of the voltage hold test at 4 V for the micro-supercapacitor device. As can be seen, a capacitance loss of approximately 25% occurs after 300 h. This tendency confirms that a high cell voltage of 4 V can be applied for SiNWs micro-supercapacitors due to its remarkable stability after hundreds of hours. Accordingly, EIS analysis and voltammetry characteristics after galvanostatic cycling have shown a vertical line and rectangular shape, respectively, displaying once more a pure capacitive behavior as seen in Figure 5c and d. Additionally, an excellent coulombic efficiency ( $\eta$ ) defined as the ratio between the discharge and charge time was observed during the cycling with a value of  $\sim 99\%$  showing the complete reversibility of charge storage based on electrical double layer capacitance. The morphology of the SiNWs after cycling was examined by using SEM images according to Figure 5e. As can be seen, the structure of SiNWs was remained unchanged even after millions of successive charge-discharge cycles presenting no degradation of the morphology of SiNWs, thus, the morphology was comparable to those observed in Figure 1a and b corresponding to SiNWs as grown (e.g. not cycled in an electrochemical device).

The results provided in this work demonstrate that  $\text{PYR}_{13}\text{TFSI}$  is an efficient electrolyte to be employed as supercapacitor. The performance of SiNWs in  $\text{PYR}_{13}\text{TFSI}$  can be found as a promising approach in the Si-based microelectronics industry for the fabrication of nanoelectronic devices where a high power density and long life cycle are required.

## Conclusion

Symmetric supercapacitors based on nanostructured SiNWs electrodes ( $L=50 \mu\text{m}$  and  $\varnothing=50 \text{ nm}$ ) were characterized using an ionic liquid ( $\text{PYR}_{13}\text{TFSI}$ ) as electrolyte at room temperature. The device exhibited an excellent capacitive behavior with a maximal power density of  $182 \text{ mW cm}^{-2}$  and a specific energy of  $0.19 \text{ mJ cm}^{-2}$  using an electrochemical window of 4 V. These high values were attributed

to the smart combination of several key qualities such as the high working voltage reached in this study due to the use of  $\text{PYR}_{13}\text{TFSI}$  as electrolyte (4 V), high active surface of the nanostructured silicon (SiNWs) and finally, the great compatibility between the electrode and the electrolyte. Moreover, the device provides an excellent stability after  $8 \times 10^6$  galvanostatic charge-discharge cycles with a loss of capacitance of only 25%. The results of this study were compared with those from micro-supercapacitors based on carbon demonstrating that SiNWs micro-supercapacitors can be applicable to different electronic technological applications according to the improvements reported in this work in terms of cycling stability and power density.

## Acknowledgments

The authors acknowledge the CEA for financial support of this work. This project has received funding from the European Union's Seventh Program for Research, Technological Development and Demonstration under Grant agreement no. 309143 (2012-2015).

## References

- [1] K.-Q. Peng, X. Wang, L. Li, Y. Hu, S.-T. Lee, *Nano Today* 8 (2013) 75-97.
- [2] M.R. Zamfir, H.T. Nguyen, E. Moya, Y.H. Lee, D. Pribat, *J. Mater. Chem. A* 1 (2013) 9566-9586.
- [3] F. Thissandier, P. Gentile, N. Pauc, E. Hadji, A. Le Comte, O. Crosnier, G. Bidan, S. Sadki, T. Brousse, *Electrochemistry* 81 (2013) 777-782.
- [4] F. Thissandier, A. Le Comte, O. Crosnier, P. Gentile, G. Bidan, E. Hadji, T. Brousse, S. Sadki, *Electrochem. Commun.* 25 (2012) 109-111.
- [5] F. Thissandier, N. Pauc, T. Brousse, P. Gentile, S. Sadki, *Nanoscale Res. Lett.* 8 (2013) 38.
- [6] J.W. Choi, J. McDonough, S. Jeong, J.S. Yoo, C.K. Chan, Y. Cui, *Nano Lett.* 10 (2010) 1409-1413.
- [7] J.P. Alper, S. Wang, F. Rossi, G. Salviati, N. Yiu, C. Carraro, R. Maboudian, *Nano Lett.* 14 (2014) 1843-1847.
- [8] L. Gu, Y. Wang, Y. Fang, R. Lu, J. Sha, *J. Power Sources* 243 (2013) 648-653.
- [9] J.P. Alper, M.S. Kim, M. Vincent, B. Hsia, V. Radmilovic, C. Carraro, R. Maboudian, *J. Power Sources* 230 (2013) 298-302.
- [10] J.P. Alper, A. Gutes, C. Carraro, R. Maboudian, *Nanoscale* 5 (2013) 4114-4118.
- [11] Y. Cui, C.M. Lieber, *Science* 291 (2001) 851-853.
- [12] B. Tao, J. Zhang, F. Miao, S. Hui, L. Wan, *Electrochim. Acta* 55 (2010) 5258-5262.
- [13] F. Lu, M. Qiu, X. Qi, L. Yang, J. Yin, G. Hao, X. Feng, J. Li, J. Zhong, *Appl. Phys. A* 104 (2011) 545-550.
- [14] J.P. Alper, M. Vincent, C. Carraro, R. Maboudian, *Appl. Phys. Lett.* 100 (2012) 163901.
- [15] M. Armand, F. Endres, D.R. MacFarlane, H. Ohno, B. Scrosati, *Nat. Mater.* 8 (2009) 621-629.
- [16] L.G. Bettini, M. Galluzzi, A. Podestà, P. Milani, P. Piseri, *Carbon* 59 (2013) 212-220.
- [17] L. Demarconnay, E.G. Calvo, L. Timperman, M. Anouti, D. Lemordant, E. Raymundo-Pinero, A. Arenillas, J. A. Menéndez, F. Béguin, *Electrochim. Acta* 108 (2013) 361-368.
- [18] P. Huang, D. Pech, R. Lin, J.K. McDonough, M. Brunet, P.-L. Taberna, Y. Gogotsi, P. Simon, *Electrochem. Commun.* 36 (2013) 53-56.

- 1 [19] L. Timperman, P. Skowron, A. Boisset, H. Galiano,  
D. Lemordant, E. Frackowiak, F. Béguin, M. Anouti, *Phys.*  
3 *Chem. Chem. Phys.* 14 (2012) 8199-8207.
- 5 [20] E. Frackowiak, G. Lota, J. Pernak, *Appl. Phys. Lett.* 86 (2005)  
164104.
- 7 [21] F. Thissandier, L. Dupré, P. Gentile, T. Brousse, G. Bidan,  
D. Buttard, S. Sadki, *Electrochim. Acta* 117 (2014) 159-163.
- 9 [22] A. Lewandowski, A. Swiderska-Mocek, *J. Power Sources* 194  
(2009) 601-609.
- 11 [23] V. Ruiz, T. Huynh, S.R. Sivakkumar, A.G. Pandolfo, *RSC Adv.* 2  
(2012) 5591-5598.
- 13 [24] P. Gentile, A. Solanki, N. Pauc, F. Oehler, B. Salem, G. Rosaz,  
T. Baron, M. Den Hertog, V. Calvo, *Nanotechnology* 23 (2012)  
215702.
- 15 [25] F. Oehler, P. Gentile, T. Baron, P. Ferret, *Nanotechnology* 20  
(2009) 475307.
- [26] D. Weingarh, H. Noh, A. Foelske-Schmitz, A. Wokaun, R. Kötz,  
*Electrochim. Acta* 103 (2013) 119-124.
- [27] D. Weingarh, A. Foelske-Schmitz, R. Kötz, *J. Power Sources*  
225 (2013) 84-88.
- [28] H. Durou, D. Pech, D. Colin, P. Simon, P.-L. Taberna, M. Brunet,  
*Microsyst. Technol.* 18 (2012) 467-473.
- [29] P.L. Taberna, P. Simon, J.F. Fauvarque, *J. Electrochem. Soc.*  
150 (2003) A292-A300.
- [30] D. Pech, M. Brunet, H. Durou, P. Huang, V. Mochalin,  
Y. Gogotsi, *Nat. Nanotechnol.* 5 (2010) 651-654.
- [31] M. Beidaghi, Y. Gogotsi, *Energy Environ. Sci.* 7 (2014) 867-884.
- [32] J.R. McDonough, J.W. Choi, Y. Yang, F. La Mantia, Y. Zhang,  
Y. Cui, *Appl. Phys. Lett.* 95 (2009) 243109.
- [33] J. Bae, M.K. Song, Y.J. Park, J.M. Kim, M. Liu, Z.L. Wang,  
*Angew. Chem. Int. Ed.* 50 (2011) 1683-1687.